Two-Dimensional Fourier Transform Ion Cyclotron Resonance Mass Spectrometry/Mass Spectrometry with Stored-Waveform Ion Radius Modulation

Charles W. Ross, III, Shenheng Guan, Peter B. Grosshans,† Tom L. Ricca,‡ and Alan G. Marshall*,§

Contribution from the Department of Chemistry, The Ohio State University, 120 West Eighteenth Avenue, Columbus, Ohio 43210

Received March 4, 1993

Abstract: A fundamentally new two-dimensional Fourier transform ion cyclotron resonance mass spectrometry experiment, SWIM ("stored-waveform ion modulation") 2D-FT/ICR MS/MS, is described. Prior encodement of the second dimension by use of two identical excitation waveforms separated by a variable delay period (analogous to 2D-NOESY NMR) is replaced by a new encodement in which each row of the two-dimensional data array is obtained by use of a single stored excitation waveform whose frequency-domain magnitude spectrum is a sinusoid whose frequency increases from one row to the next. In the two-dimensional mass spectrum, the conventional one-dimensional FT/ICR mass spectrum appears along the diagonal, and each off-diagonal peak corresponds to an ion-neutral reaction whose ionic components may be identified by horizontal and vertical projections to the diagonal spectrum. Fragmentation due to (e.g.) collision-induced dissociation results in peaks on only one side of the diagonal, whereas bidirectional ion–molecule reactions result in peaks on both sides of the diagonal. All ion–molecule reactions in a gaseous mixture may be identified from a single 2D-FT/ICR MS/MS experiment, without any prior knowledge of the system.

Introduction

Fourier transform ion cyclotron resonance mass spectrometry (FT/ICR/MS) is the most versatile technique for identifying ion–molecule reaction pathways and quantifying ion-molecule reaction kinetics, equilibria, and energetics in the absence of solvent (i.e., the gas phase). As itemized in several recent reviews,[1-18] FT/ICR/MS has analytically important features: speed (~1 s per spectrum); ultrahigh mass resolving power and ultrahigh mass accuracy; low-volatility samples (10^{-9} Torr), MS/MS/··· with one spectrometer, wide mass range ($1 \le m \le 32\,000$ u for singly-charged ions);[19,20] positive and/or negative ion detection;[21] multiple ion sources for analysis of involatile substances and mixtures; and simultaneous multiple-ion monitoring.

One-Dimensional ICR MS/MS. Of particularly high interest to chemists is the high-resolution FT/ICR mass spectrometric detection of ions trapped for extended periods (up to 10^6 collisions), during which ion-molecule reaction chemistry may be observed and quantitated. From the cyclotron equation (S.I. units)

$$\omega_c = \frac{qB}{m} \qquad (1)$$

in which ω_c is the cyclotron frequency of ions of mass m and charge q moving in a magnetic field B, it is clear that the mass-to-charge ratio of a given ion may be accessed according to its cyclotron frequency. Thus, just as populations of nuclear spin energy levels may be perturbed by selective irradiation at the appropriate transition frequency in so-called "double-resonance" nuclear magnetic resonance (NMR) experiments,[22] ion populations may be altered by selective "double-resonance" irradiation at ω_c to "heat" ions of the corresponding mass-to-charge ratio m/z (m in u, z in number of elementary charges per ion) to higher translational energy, thereby changing the relative abundance of those ions and any others connected to the irradiated ions by ion-molecule reactions.[23] The "double-resonance" ICR experiment is a form of what has later been denoted as "tandem mass spectrometry"[24] or MS/MS. However, in both types of one-dimensional experiments, only one spin–spin (or parent ion–product ion) connection may be established at a time.

One-Dimensional FT/ICR MS/MS. The introduction of broad-band excitation and detection followed by Fourier transform

* To whom correspondence should be addressed.
† Current address: Exxon Research and Engineering Company, Room LF148, Route 22 East, Annandale, NJ 08801.
‡ OSU Campus Chemical Instrument Center.
§ Also a member of the Department of Biochemistry.

(1) Marshall, A. G. In *IUCCP Symposium*; Texas A&M University Press: College Station, TX, 1985; pp 111–134.
(2) *Fourier Transform Mass Spectrometry: Evolution, Innovation, and Applications*; Buchanan, M. V., Ed.; American Chemical Society: Washington, D.C., 1987; Vol. 359.
(3) Sharpe, P.; Richardson, D. E. *Coord. Chem. Rev.* **1989**, *93*, 59–85.
(4) Wanczek, K.-P. *Int. J. Mass Spectrom. Ion Processes* **1989**, *95*, 1–38.
(5) Wilkins, C. L.; Chowdhury, A. K.; Nuwaysir, L. M.; Coates. M. L. *Mass Spectrom. Rev.* **1989**, *8*, 67–92.
(6) Freiser, B. S. In *Bonding Energetics in Organometallic Compounds*; Marks, T. J., Ed.; American Chemical Society: Washington, D.C., 1990; Vol. 428; pp 55–69.
(7) Laude, D. A., Jr.; Hogan, J. D. *TM, Tech. Mess.* **1990**, *57*, 155–159.
(8) *Lasers in Mass Spectrometry*; Lubman, D. M., Ed.; Oxford University Press: New York, 1990.
(9) Nibbering, N. M. M. *Acc. Chem. Res.* **1990**, *23*, 279–285.
(10) Asamoto, B.; Dunbar, R. C. *Analytical Applications of Fourier Transform Ion Cyclotron Resonance Mass Spectrometry*; VCH: New York, 1991.
(11) Campana, J. E. In *Proceedings SPIE, Applied Spectroscopy in Material Science*; The International Society for Optical Engineering: Bellingham, WA, 1991; pp 138–149.
(12) Eller, K.; Schwarz, H. *Chem. Rev.* **1991**, *91*, 1121–1177.
(13) Marshall, A. G.; Grosshans, P. B. *Anal. Chem.* **1991**, *63*, 215A-229A.
(14) Nuwaysir, L. M.; Wilkins, C. L. In *Proceedings SPIE, Applied Spectroscopy in Material Science*; The International Society for Optical Engineering: Bellingham, WA, 1991; pp 112–123.
(15) Dunbar, R. C. *Mass Spectrom. Rev.* **1992**, *11*, 309–339.
(16) Marshall, A. G.; Schweikhard, L. *Int. J. Mass Spectrom. Ion Processes* **1992**, *118/119*, 37–70.
(17) Buchanan, M. V.; Hettich, R. L. *Anal. Chem.* **1993**, *65*, 245A–259A.
(18) Schweikhard, L.; Marshall, A. G. *J. Am. Soc. Mass Spectrom.* **1993**, *4*, 433–452.
(19) Schweikhard, L.; Alber, G. M.; Marshall, A. G. *J. Am. Soc. Mass Spectrom.* **1993**, *4*, 177–181.
(20) Lebrilla, C. B.; Wang, D. T.-S.; Hunter, R. L.; McIver, R. T., Jr. *Anal. Chem.* **1990**, *62*, 878–880.
(21) Gorshkov, M. V.; Guan, S.; Marshall, A. G. *Rapid Commun. Mass Spectrom.* **1992**, *6*, 166–172.
(22) Baldeschwieler, J. D.; Randall, E. W. *Chem. Rev.* **1963**, *63*, 81–110.
(23) Anders, L. R.; Beauchamp, J. L.; Dunbar, R. C.; Baldeschwieler, J. D. *J. Chem. Phys.* **1966**, *45*, 1062–1063.
(24) *Tandem Mass Spectrometry*; McLafferty, F. W., Ed.; Wiley: New York, 1983.

0002-7863/93/1515-7854$04.00/0

data reduction revolutionized infrared, NMR, and ICR mass spectrometry, by making it possible to acquire a full-range spectrum in the time previously required to scan through a single peak.[25] In all three cases, roughly comparable advantages in speed (factor of 10^4) or signal-to-noise ratio (factor of 10^2) were demonstrated. Fourier transform ion cyclotron resonance mass spectrometry (FT/ICR/MS) provided the unique additional advantage of higher spectral resolution and (especially) higher mass accuracy (factor of up to 10^7).[26] Following the advent of Fourier transform techniques in NMR[27] and ICR,[28,29] the "double-resonance" experiment was immediately improved by simultaneous detection of *all* spins (or "product" ions) connected to a given irradiated spin (or "parent" ion[30]), due to the multiplex advantage of FT data reduction.[25] In ICR, the MS/MS method is further improved by prior selective radial ejection of ions of all but the "parent" ion m/z of interest, optimally by use of "SWIFT" (stored-waveform excitation based on inverse Fourier transform of the desired frequency-domain excitation spectrum).[31,32]

Two-Dimensional FT Spectroscopy. In one-dimensional FT/ICR MS/MS, a given ion fragmentation or reaction pathway is established by (a) isolating the parent ions of interest (by ejecting ions of all other m/z values); (b) (optionally) resonantly cyclotron exciting those parent ions to a larger cyclotron orbital radius and thus higher kinetic energy; (c) waiting for a fixed period to allow for collision-induced dissociation and/or ion-molecule reactions; and finally (d) detecting and Fourier transforming the time-domain response to a broad-band excitation of ions throughout the m/z range of interest. Although such a scheme achieves multiplex detection of all product ions deriving from parent ions of a given m/z, only one parent m/z is interrogated at a time, and the experiment must be repeated for each parent m/z of interest. Thus, the approach is feasible for sparse spectra of ions of relatively few m/z values but is inefficient for complex mixtures such as crude oil distillates which may contain thousands of comparably abundant components.

One is therefore led to seek a two-dimensional MS/MS experiment with multiplexing with respect to both parent and product ions. Again, we look to NMR, where a second revolution followed the introduction of various two-dimensional FT/FT experiments,[33] principally COSY[34] and NOESY.[35] The appeal of 2D-FT/NMR is obvious: it is possible to establish the "couplings" (e.g., "scalar" or "dipolar") between two spins, even in a highly overlapped spectrum, from a two-dimensional contour plot in which the spectrum itself is either dispersed along the diagonal (NOESY) or visualized by projection (COSY), and the couplings are manifested as off-diagonal peaks whose horizontal and vertical projections to the diagonal identify the chemical shifts of the two coupled spins. The COSY 2D-FT/NMR idea has since been extended to microwave pure rotational[36] and electron paramagnetic resonance[37] spectroscopy.

The fundamental requirements of a 2D-FT experiment are the generation of some sort of "coherence" (i.e., all spins or ions moving together) and a means for "modulating" that coherence sinusoidally to generate a second FT dimension. If the coupling between two spins is inherently coherent (as in "scalar", or J-coupling, which is the same for all molecules in the sample), then a 90° pulse generates an observable signal whose amplitude is modulated by the J-coupling during a subsequent "evolution period", leading to the COSY-type 2D-FT/NMR experiment. Alternatively, even though spin populations are coupled by inherently incoherent dipole–dipole or chemical-exchange interactions, it is possible to modulate the spin populations with a coherent excitation (which is the same for all molecules in the sample), leading to a NOESY-type 2D-FT/NMR experiment. Because ion-molecule reactions represent an inherently incoherent coupling (i.e., different for different ions in the sample), there is no ICR analog of COSY 2D-FT/NMR experiments. However, following the demonstration of the ICR analog of a coherent 180° NMR pulse,[38] Pfändler *et al.* were led to develop an ICR analog[39-41] to NOESY 2D-FT/NMR, as discussed below. The ICR analog of NMR spin "coupling" is ion–neutral reaction or collisional dissociation.

2D-FT/ICR MS/MS: Parent Ion Cyclotron Radius Modulation. The key concept for 2D FT/ICR is that if, in proceeding through a series of otherwise identical experiments, one can somehow sinusoidally modulate the ICR orbital radius (and hence the speed) of parent ions of one m/z value, then the yield of product ions of different m/z ratios formed by ion–neutral collisions or reactions of that parent ion will be modulated at that same frequency [because, in the hard-sphere collision limit (see below) faster-moving parent ions will collide with more neutrals during a given time period].[42] If it can then be arranged that parent ions of different m/z can be modulated at different frequencies from one experiment to the next, then the parent–product connections can be established by determining which product ion abundances are modulated at the frequencies of which parent ions, by taking a (second) FT of the frequency-modulated series of spectra. In this way, one achieves multiplexing with respect to the parent ions as well as the product ions, in a single automated experiment. Given the strong dependence of ion-molecule reaction rates on kinetic energy, especially for endothermic (CID) reactions, it is in principle preferable to modulate ion kinetic energy rather than ion radius (velocity) (see Results and Discussion).

Parent Ion Cyclotron Radius Modulation by Two Excitation Pulses Separated by a Variable Delay Period. The key concept for 2D in the Bodenhausen–Gäumann 2D-FT/ICR experiment[39-41] is that the parent ion cyclotron orbital radius is modulated from one event sequence to the next by linearly incrementing the delay period, t_1, between two identical radiofrequency single-frequency (or frequency-sweep) excitation events (see Figure 1). The first excitation is designed to drive ions radially outward from the center of the ion trap partway to one of the sides. Then, if t_1 is exactly an odd integer multiple of half a period of the ICR frequency of a given parent ion, that parent ion will be de-excited by the second pulse back to a near-zero ICR radius before the ion-molecule reaction period. However, if t_1 is exactly an integer

(25) Marshall, A. G.; Verdun, F. R. *Fourier Transforms in NMR, Optical, and Mass Spectrometry: A User's Handbook*; Elsevier: Amsterdam, The Netherlands, 1990.
(26) Gorshkov, M. V.; Alber, G. M.; Schweikhard, L.; Marshall, A. G. *Phys. Rev. A* **1993**, *47*, 3433–3436.
(27) Ernst, R. R.; Anderson, W. A. *Rev. Sci. Instrum.* **1966**, *37*, 93.
(28) Comisarow, M. B.; Marshall, A. G. *Chem. Phys. Lett.* **1974**, *25*, 282–283.
(29) Comisarow, M. B.; Marshall, A. G. *Chem. Phys. Lett.* **1974**, *26*, 489–490.
(30) Comisarow, M. B.; Grassi, V.; Parisod, G. *Chem. Phys. Lett.* **1978**, *57*, 413–416.
(31) Marshall, A. G.; Wang, T.-C. L.; Ricca, T. L. *J. Am. Chem. Soc.* **1985**, *107*, 7893–7897.
(32) Marshall, A. G.; Wang, T.-C. L.; Chen, L.; Ricca, T. L. In *American Chemical Society Symposium Series*; Buchanan, M. V., Ed.; American Chemical Society: Washington, D. C., 1987; Vol. 359, pp 21–33.
(33) Ernst, R. R.; Bodenhausen, G.; Wokaun, A. *Principles of Nuclear Magnetic Resonance in One and Two Dimensions*; Oxford University Press: London, 1987.
(34) Bax, A.; Freeman, R. *J. Magn. Reson.* **1981**, *44*, 542–561.
(35) Bodenhausen, G.; Ernst, R. R. *J. Am. Chem. Soc.* **1982**, *104*, 1304–1309.
(36) Vogelsanger, B.; Andrist, M.; Bauder, A. *Chem. Phys. Lett.* **1988**, *144*, 180–186.
(37) Gorcester, J.; Freed, J. H. *J. Chem. Phys.* **1988**, *88*, 4678–4693.
(38) Marshall, A. G.; Wang, T.-C. L.; Ricca, T. L. *Chem. Phys. Lett.* **1984**, *105*, 233–236.
(39) Pfändler, P.; Bodenhausen, G.; Rapin, J.; Houriet, R.; Gäumann, T. *Chem. Phys. Lett.* **1987**, *138*, 195–200.
(40) Pfändler, P.; Bodenhausen, G.; Rapin, J.; Walser, M.-E.; Gäumann, T. *J. Am. Chem. Soc.* **1988**, *110*, 5625–5628.
(41) Bensimon, M.; Zhao, G.; Gäumann, T. *Chem. Phys. Lett.* **1989**, *157*, 97–100.
(42) Guan, S.; Jones, P. R. *J. Chem. Phys.* **1989**, *91*, 5291–5295.

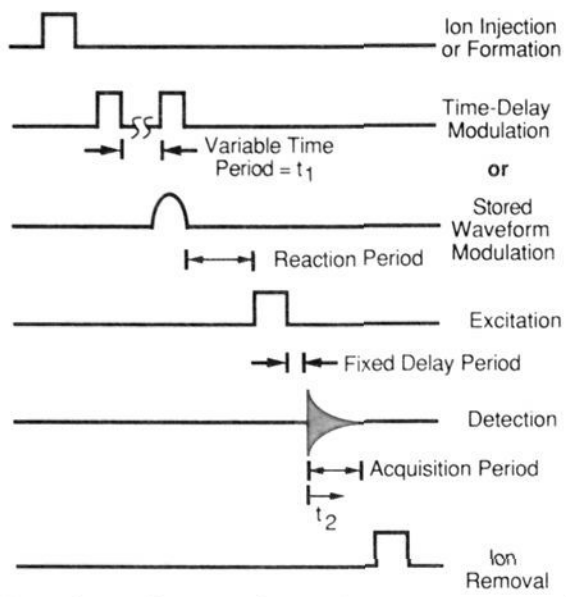

Figure 1. Two alternative experimental event sequences for 2D-FT/ICR/MS. Ion formation (top row) is followed by an excitation which modulates the parent ion cyclotron radii according to their ion cyclotron frequencies, either by application of two identical excitation waveforms separated by a delay period whose duration is incremented linearly from one data acquisition to the next (second row) or by application of each of a series of stored waveforms (third row). Following a reaction period during which product ions are formed with abundances determined by the parent ion cyclotron radii established in the previous event, conventional broad-band excitation and detection generate a time-domain response. Finally, ions are removed, and succeeding data sets are acquired, either for various delay periods between the two-pulse excitation or for various SWIFT modulation waveforms, and the two-dimensional array is subjected to two-dimensional FT to generate a 2D-FT/ICR mass spectrum (see text).

multiple of one period of the parent ICR frequency, then the second pulse will excite those parent ions out to twice the ICR radius reached at the end of the first pulse. (A one-dimensional version of the Bodenhausen–Gäumann experiment was later used by Russell for mass-selective axialization of previously broad-band-excited ions in coherent cyclotron orbits,[43] and a more general axialization method based on quadrupolar excitation has since been demonstrated for FT/ICR/MS.[44,45]) Since the accumulated phase during the delay period, t_1, is simply $\omega_p t_1$, where ω_p is the ICR frequency of the parent ion, it is clear that the radius of parent ions in successive event sequences will be modulated at frequency ω_p as a function of t_1, as t_1 is incremented from one event sequence to the next. The number of product ions produced after a fixed ion-neutral reaction period, t_{rx}, from those parent ions will therefore also be modulated at frequency ω_p. Thus, the parent ion speed modulation is converted to a product ion population modulation by means of ion-molecule reactions. Next, conventional broad-band excitation and detection followed by Fourier transformation yield an FT/ICR mass spectrum for each delay period, t_1. Finally, a second Fourier transform with respect to the t_1-axis then yields the full two-dimensional display. (These stages will be illustrated below for the presently proposed modulation method.)

Parent Ion Cyclotron Radius Direct Modulation by Stored-Waveform Excitation. Here we demonstrate experimentally for the first time a second means for parent ion radius modulation, based on use of a single excitation time-domain waveform whose magnitude varies sinusoidally (rather than is constant) with frequency, as shown in Figure 2 ("SWIM" is our acronym for "stored-waveform ion modulation"). (Each time-domain excitation waveform is produced by inverse FT[31,32,46–50] of the

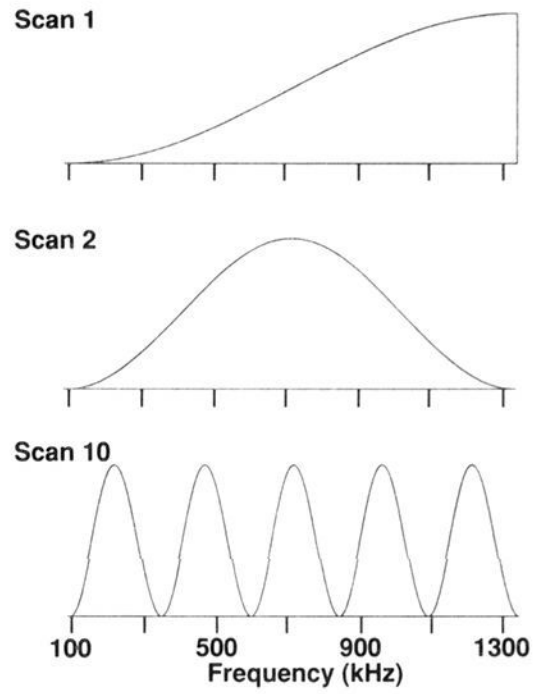

Figure 2. SWIFT magnitude-mode spectra (see eq. 3) of several parent ion modulation waveforms, for $j = 1, 2$, and 10. Note that the excitation amplitude for ions of the highest cyclotron frequency, 1333.0 kHz, is modulated the fastest in proceeding from one waveform to the next, whereas the excitation amplitude for ions of the lowest cyclotron frequency, 100 kHz, is not modulated at all from one waveform to the next. The mass-to-charge ratio range corresponding to these ion cyclotron frequencies is $34.8 < m/z < 463$ ($B \approx 3.02$ T).

corresponding frequency-domain magnitude spectrum in Figure 2.) In proceeding from one experiment to the next (see Theory), we vary the frequency of sinusoidal excitation magnitude across the spectrum (scan 1, 2, ..., 10 in Figure 2). The net result is the same as that of the Bodenhausen–Gäumann modulation, with the advantage that we can more easily vary the modulation from one scan to the next because the excitation period is fixed and does not need to be varied in inconveniently short increments (as is the case for the Bodenhausen–Gäumann experiment for large spectral bandwidth). Although the presently proposed method was conceived independently (and previously) by Williams and McLafferty,[51] we are the first to reduce it to practice. In this paper, we proceed to develop the (simple) theory of the SWIM experiment and then go on to demonstrate its value experimentally on two simple chemical systems.

Comparison to Prior Hadamard/FT 2D-ICR/MS. Before proceeding to the present experiments, we digress briefly to compare the presently proposed FT/ICR MS/MS method to the prior Hadamard transform 2D ICR experiment (henceforth denoted as HT/FT/ICR MS/MS). As originally devised and demonstrated by Williams and McLafferty,[52,53] HT/FT/ICR MS/MS replaces the present stored-waveform ion modulation (SWIM) of Figure 2 with a "comb" excitation spectrum whose "teeth" are positioned to excite equally a particular combination of about half of the possible parent ions of interest. In proceeding from one experiment to the next, one chooses an appropriately different (and linearly independent) combination of parent ions. The "Hadamard" aspect simply prescribes the elements of the "code" which determines which parent ions are excited in which experiment. After N experiments (corresponding to N different linear combinations of the original N parent ions), a Hadamard (rather than Fourier) "decoding" produces a 2D display consisting of N spectra, each of which is the spectrum of product ions resulting from excitation of just one parent ion. The HT/FT approach requires a smaller minimum number of scans than the FT/FT

(43) Kerley, E. L.; Russell, D. H. *Anal. Chem.* **1989**, *61*, 53–57.
(44) Schweikhard, L.; Guan, S.; Marshall, A. G. *Int. J. Mass Spectrom. Ion Processes* **1992**, *120*, 71–83.
(45) Guan, S.; Marshall, A. G. *J. Chem. Phys.* **1993**, *98*, 4486–4493.
(46) Chen, L.; Wang, T. C. L.; Ricca, T. L.; Marshall, A. G. *Anal. Chem.* **1987**, *59*, 449–454.
(47) Guan, S. *J. Chem. Phys.* **1989**, *91*, 775–777.
(48) Guan, S.; McIver, R. T., Jr. *J. Chem. Phys.* **1990**, *92*, 5841–5846.
(49) Guan, S. *J. Chem. Phys.* **1990**, *93*, 8442–8445.
(50) Grosshans, P. B.; Marshall, A. G. *Anal. Chem.* **1991**, *663*, 2057–2061.
(51) Williams, E. R.; McLafferty, F. W. Unpublished results.
(52) McLafferty, F. W.; Stauffer, D. B.; Loh, S. Y.; Williams, E. R. *Anal. Chem.* **1987**, *59*, 2212–2213.
(53) Williams, E. R.; Loh, S. Y.; McLafferty, F. W.; Cody, R. B. *Anal. Chem.* **1990**, *62*, 698–703.

approach, because the Hadamard experiment requires interrogation only at the ICR frequencies of the parent ions, rather than interrogation at all of the discrete frequencies in the spectrum.

However, it is fair to note that although HT/FT methods have been available in NMR for more than a decade,[54] FT/FT data reduction[33] is overwhelmingly preferred. We believe that the same will be true for 2D-FT/ICR MS/MS. First, Hadamard (or FT) techniques are most efficient when the number of data points, n, is $2^n - 1$ (or 2^n for FT), n = an integer. Although it is relatively easy to choose the number of time-domain data points to be 2^n, it is not in general true that the number of parent ions in the spectrum will match the $2^n - 1$ value. Of course, in the Hadamard method, n is the number of parent ions, which is in general much less than the number of spectral data points (n in the FT case). However, 2D-FT closes the gap as the spectrum becomes denser (as for complex mixtures of many components), particularly at high mass (where the exact masses do not necessarily cluster near the nominal mass). Moreover, the 2D-FT peak heights more accurately reflect the relative ion-molecule reaction rate constants (because the 2D-FT data are sampled from a *range* of ion translational energies) than the HT (which, for optimal SNR, would be conducted at very high translational energy where CID is nearly collision-limited for all species). Also, the Hadamard technique requires that each parent ion be excited to its optimal radius (because the kinetic energy-dependence of different ion-molecule reactions is different) to produce product ions (information generally not known in advance of the experiment). The FT/FT approach, on the other hand, inherently depends on *modulation* of the parent ion energy over a range of kinetic energy and thus should be more generally applicable. It is important to note that the Hadamard technique requires prior knowledge of which parent ion m/z values are to be examined, whereas the FT method requires no such prior knowledge. Finally, in the FT/FT experiment, all parent ions (rather than approximately half) are interrogated in each scan. Comparison of signal-to-noise ratio for HT/FT and FT/FT experiments is thus a complex issue which is currently under investigation.

Theory

Parent Ion Cyclotron Radius Modulation by Excite–(Variable Delay)–Excite Sequence. The prior cyclotron radius modulation method employed by Pfändler *et al.*[39-41] uses two identical single-frequency or frequency-sweep events separated by a time period, t_1, which is incremented to generate successive rows of a two-dimensional signal, $s(t_1,t_2)$, as shown in Figure 1. The final (parent) ion cyclotron radius following the excite–delay–excite sequence therefore varies sinusoidally as a function of t_1. If the two excitation waveforms are identical, then the sinusoidal radius modulation frequency for parent ions of a given m/z is simply the cyclotron frequency corresponding to that m/z value. In practice, Pfändler *et al.* changed the phase of their second excitation with respect to the first in order to achieve effectively heterodyne detection in the t_1 domain,[40] so that their parent ion cyclotron radius was modulated at the difference in frequency between their radiofrequency carrier (for single-frequency excitation) or highest sweep frequency (for frequency-sweep excitation) and the parent ion cyclotron frequency.

Parent Ion Cyclotron Radius Modulation by a Series of Single-Event SWIFT Excitations. Once one recognizes that the end result of the excite–delay–excite sequence is to produce a sinusoidal excitation vs frequency spectrum of the type shown in a given row of Figure 2, then it is clear that, because the ICR system is highly linear,[50,55] the same result could be obtained simply by irradiation with a time-domain waveform obtained by inverse Fourier transformation of the desired sinusoidal excitation spectrum of the appropriate frequency. One then simply increments the sinusoid frequency in proceeding from one event sequence to the next. Because the parent ion radius is modulated by stored-waveform excitation, we propose the acronym SWIM (stored-waveform ion modulation) for this technique.

To satisfy the Nyquist criterion with the minimum number of experiments in the t_1 dimension, we choose a frequency-domain representation for the jth SWIM excitation waveform magnitude, $M_j(\nu)$, given simply by

$$M_j(\nu) = \frac{1 + \sin\left(2\pi\nu_{\text{modulation}} j\Delta t - \frac{\pi}{2}\right)}{2}; j = 1, 2, ..., n \tag{2a}$$

in which

$$\nu_{\text{modulation}} = \nu_{\text{high}}\left(\frac{\nu - \nu_{\text{low}}}{\nu_{\text{high}} - \nu_{\text{low}}}\right); 0 < \nu_{\text{modulation}} < \nu_{\text{high}} \tag{2b}$$

and $\Delta t = 1/2\nu_{\text{high}}$ is the sampling interval in the t_1 dimension. Thus, ν_{high} represents the Nyquist (modulation) frequency in the t_1 dimension, so that the sampling frequency is $2\nu_{\text{high}}$ in the t_1 dimension. Clearly, $0 \le M_j(\nu) \le 1$. Substitution of eq 2b and $\Delta t = 1/2\nu_{\text{high}}$ into eq 2a yields eq 3, which was used to generate

$$M_j(\nu) = \frac{1 + \sin\left(j\pi\left(\frac{\nu - \nu_{\text{low}}}{\nu_{\text{high}} - \nu_{\text{low}}}\right) - \frac{\pi}{2}\right)}{2} \tag{3}$$

the SWIFT ion modulation waveforms. For example, for $j = 1$, the SWIFT excitation waveform varies sinusoidally by half a period over the excitation frequency range (Figure 2, scan 1). For $j = 2$, there is one full period over that range (Figure 2, scan 2). For $j = 3$, there are one and a half periods over the range, and so on. The parent ion modulation frequencies therefore range from 0 for ions of lowest cyclotron frequency, ν_{low}, to ν_{high} for ions of highest cyclotron frequency, ν_{high}, across the SWIFT-excited frequency range.

Specifically, $M(\nu)$ varies most rapidly (1, 0, 1, 0, 1, 0, from one row to the next) as a function of j at the high-frequency limit of the range (ν_{high}), whereas $M(\nu)$ is constant (0, 0, 0, 0, ..., from one row to the next) at the low-frequency limit of the range (ν_{low}). At the midpoint frequency in the range, the excitation values vary as ($^1/_2$, 1, $^1/_2$, 0, $^1/_2$, 1, etc.). Thus, the cyclotron radius for ions of any given m/z ratio is modulated at a unique modulation frequency. The modulation of eq 3 is such that ions of *higher* cyclotron frequency will have a *higher* modulation frequency. If the sine function in eq 3 were replaced by a cosine, then ions of *higher* cyclotron frequency would have a *lower* modulation frequency.

Experimental Section

Analytical reagent-grade acetone was obtained from Mallinckrodt Specialty Chemicals Co. (Paris, Kentucky). Pyrrolidine and 3-methylpyridine were obtained from Aldrich Chemical Co., Inc. (Milwaukee, WI). All chemicals were used as supplied except for multiple freeze–pump–thaw cycles to degas the sample.

The stored-waveform ion modulation (SWIM) 2D/FT/FT/ICR/MS experiments were implemented on a dual-trap FTMS-2000 FT/ICR mass spectrometer (Extrel FTMS Millipore Inc., Madison, WI), operated at 3.0 T, equipped with Helix Technology CryoTorr-8 2000 L/s cryopumps (Waltham, MA) for both source and analyzer vacuum chambers, with two 4.76-cm cubic traps in a standard dual-trap configuration. The mass spectrometer was controlled by a Nicolet 1280 computer. Each gaseous sample was introduced through a leak valve (Model 951-5100, Varian, Palo Alto, CA) connected to the batch inlet system of the instrument. All experiments were conducted in the "source" compartment of the dual trap.

(54) Blümich, B.; Ziessow, D. *J. Magn. Reson.* **1982**, *46*, 385–405.
(55) Guan, S. *J. Am. Soc. Mass Spectrom.* **1991**, *2*, 483–486.

A 1280 computer Fortran program was written to produce the modulation waveform data. A series of 512 magnitude-mode excitation spectra was generated from eq 3, with quadratically modulated phase,[46,47] and inverse Fourier transformed to produce 512 SWIFT modulation waveforms of 4K data points each. Those waveforms were stored in the 1280 data system for subsequent one-at-a-time loading into the buffer memory of a home-built SWIFT module.[31] Figure 2 shows three representative frequency-domain magnitude-mode excitation profiles used to synthesize (by inverse FT) three corresponding SWIM time-domain excitation waveforms. For subsequent excitation and detection, a single flat-amplitude SWIFT excitation waveform of flat frequency-domain magnitude over the ICR frequency range of interest was generated with the same bandwidth and frequency range as those of the SWIM data sets.

For acetone ion-molecule chemistry, the experimental event sequence (Figure 1) begins with electron ionization (70 eV for 10 ms at an emission current of 4.1 μA measured just behind the filament) of acetone (10^{-6} Torr). Following a short (0.5 s) equilibration period, SWIM excitation (frequency bandwidth = 1.000 MHz; ν_{low} = 75 kHz; ν_{high} = 999.75 kHz) is applied for 2.048 ms at a maximum of 27.6 $V_{(p-p)}$, which excites ions to a maximum radius of approximately 2.8 mm,[50,55,56] and the variably excited ions are allowed to collide and/or react with neutrals for a fixed reaction period of 1.0 s, followed by SWIFT broad-band direct-mode excitation for 8.192 ms at 19.6 $V_{(p-p)}$ to excite ions to a cyclotron radius of 4.0 mm. A single transient ICR signal was direct-mode acquired (1.333 MHz Nyquist frequency for 1.54 ms to yield 4096 data points). The signal-to-noise ratio was sufficiently high that signal averaging was not required for this experiment. All ions were then removed from the ICR ion trap by successive application of +10 V to both trap electrodes and then −10 V to both trap electrodes. The time-domain digitized transient signal from this experiment constitutes one row of a two-dimensional time–time data array. The same experimental event sequence was then repeated for each of the 512 SWIM excitations to produce a two-dimensional time–time data array, $D(i,t_2)$, in which $1 \leq i \leq 512$.

The 2-D time–time data array was transferred from the 1280 computer to a PC AT-compatible computer (AT&T Model 6300+) via a home-built parallel data transfer channel which provided an 8-fold increase in the data transfer rate compared to that of a standard serial port connection. The data were converted to a FELIX (a commercial NMR data processing program from Hare Research, Inc., Seattle, WA) file format. The converted data were transferred to an IBM RISC-6000 workstation through a local network. A data processing protocol written in the FELIX microformat was used for 2D-FT data reduction (512 × 2048 data points) and display.

Each of the 512 rows of the two-dimensional time-domain data $s(t_1,t_2)$ consisting of 4096 data points was Fourier transformed with respect to the acquisition period, t_2, without apodization or zero-filling to generate a series of 512 magnitude-mode spectra $S(t_1,\omega_2)$, and the phase portion of each spectra was discarded.[42] Each of the resultant 2048 columns of $S(t_1,\omega_2)$ consisting of 512 data points was then padded with 512 zeroes and Fourier transformed with respect to the "j" index, and the resulting two-dimensional spectral array, $S(\omega_1,\omega_2)$, was recorded on an HP line plotter in magnitude mode, either as a stack plot or as two-dimensional contours of constant magnitude (1D) or power (2D).

For the pyrrolidine/3-methylpyridine experiments, the conditions were electron ionization (9 eV for 10 ms at a measured current of 12.7 μA), at equal partial pressure (2×10^{-7} Torr). A preparation delay of 20 ms and a reaction period of 150 ms were used before and after SWIM excitation, respectively. The SWIM modulation waveform parameters were frequency bandwidth = 2.666 MHz, ν_{low} = 100.0 kHz, ν_{high} = 2.600 MHz ($17.85 < m/z < 463.4$, $B \approx 3.02$ T), 4096 time-domain data to give a 0.768-ms excitation event, time-domain amplitude = 98 $V_{(p-p)}$ (see eq 3). The same excitation conditions were used for the final excitation except that the frequency-domain SWIFT magnitude spectrum was constant (rather than sinusoidal) over the excited frequency range. Ten coadded digitized (Nyquist bandwidth, 1.600 MHz) time-domain transients of 4096 data points each were acquired to increase the signal-to-noise ratio, to compensate for the reduced number of ions resulting from much lower electron beam energy (9 vs 70 eV) for pyrrolidine/3-methylpyridine compared to acetone.

For the pyrrolidine data shown in Figure 7, conditions were identical to those listed above except that the SWIFT excitation bandwidth was narrowed from 2.6666 to 1.0 MHz for both excitations, to yield higher digital spectral resolution. 4096 SWIFT data yielded a modulation-excitation event of 2.048 ms, at a 34.5-$V_{(p-p)}$ time-domain excitation amplitude. Ten 4K time-domain transients were coadded at a Nyquist bandwidth of 1 MHz for each SWIFT modulation waveform excitation.

Finally, peak areas for the one-dimensional double-resonance experiments were calculated from a simple program written in resident Extrel software. Each peak area represents the product of the peak maximum magnitude value and the full peak width at half-maximum peak height.[57,58]

Results and Discussion

Fundamental Aspects of 2D-FT/ICR MS/MS. For low-energy ion-molecule reactions, the ion-molecule reaction rate is well-described by a Langevin ion-induced dipole collision model,[59–63] for which the ion-molecule collision frequency is independent of ion speed. However, above a critical suprathermal ion speed, the reaction is better described by a hard-sphere model, for which the ion-molecule collision frequency (and thus the ion-molecule reaction rate) is directly related to ion speed.[64] For example, for N_2^+, the crossover from Langevin to hard-sphere collision mechanism occurs at an ion cyclotron orbital radius of only a few millimeters at a magnetic field of 4.7 T.[64] Since ion cyclotron orbital speed is proportional to ion cyclotron orbital radius,[25] the present SWIM technique can thus be expected to produce a sinusoidal modulation of product ion yield from sinusoidally modulated parent ion cyclotron radius, provided that the ion cyclotron radius is modulated over a range which exceeds a few millimeters.[65]

Another underlying assumption of the present scheme is that the response amplitude (i.e., ion cyclotron orbital radius) is linearly proportional to the on-resonance excitation amplitude.[50,55] Unlike NMR, for which the detected signal varies approximately as the sine of the excitation amplitude, the ICR response to dipolar radial excitation has been shown to be quite linear out to an ion cyclotron radius more than 90% of the radius of the trap,[50,66] particularly if the radiofrequency excitation field is "shimmed" to spatial homogeneity.[67] Thus, SWIFT excitation (which is based on the linear proportionality between time-domain and frequency-domain representations of an excitation waveform) is eminently suitable for use in 2D-FT/ICR MS/MS.

Monomer–Dimer Interconversion: Acetone. As our first experimental test of the SWIM 2D-FT/ICR MS/MS method, we chose the simple ion-molecule reaction system derived from electron-ionized acetone. Electron ionization generates molecular ions, M^+, which react rapidly on the ICR time scale to form protonated acetone, MH^+. MH^+ ions (m/z 59) trapped for tens of collisions with acetone neutrals (e.g., ~0.5 s at 10^{-6} Torr) react further to form abundant proton-bound dimer ions, M_2H^+ (m/z 117), by the exoergic reaction

$$MH^+ + M \rightarrow M_2H^+ \qquad (4)$$

An increase in kinetic energy of the parent MH^+ ions may actually decrease the yield of M_2H^+ ions. Conversely, the rate of collision-induced fragmentation of M_2H^+ with a neutral, N

(56) Guan, S. *J. Chem. Phys.* **1992**, *96*, 7959–7964.
(57) Liang, Z.; Marshall, A. G.; Westmoreland, D. G. *Anal. Chem.* **1991**, *63*, 815–818.
(58) Liang, Z.; Marshall, A. G. *Anal. Chem.* **1990**, *62*, 70–75.
(59) Langevin, P. *Ann. Chim. Phys.* **1905**, *5*, 245.
(60) Gioumousis, G.; Stevenson, D. P. *J. Chem. Phys.* **1958**, *29*, 294–299.
(61) Su, T.; Bowers, M. T. *Int. J. Mass Spectrom. Ion Processes* **1973**, *12*, 347.
(62) Wobschall, D.; Graham, J. R., Jr.; Malone, D. P. *Phys. Rev.* **1963**, *131*, 1565–1571.
(63) Beauchamp, J. L. *J. Chem. Phys.* **1967**, *46*, 1231–1243.
(64) Laukien, F. In *Proceedings of the 35th American Society of Mass Spectrometry Conference on Mass Spectrometry & Allied Topics*; American Society of Mass Spectrometry: Denver, CO, 1987; pp 781–782.
(65) Hop, C. E. C. A.; McMahon, T. B.; Willett, G. D. *Int. J. Mass Spectrom. Ion Processes* **1990**, *101*, 191–208.
(66) Grosshans, P. B.; Shields, P. J.; Marshall, A. G. *J. Chem. Phys.* **1991**, *94*, 5341–5352.
(67) Wang, M.; Marshall, A. G. *Anal. Chem.* **1990**, *62*, 515–520.

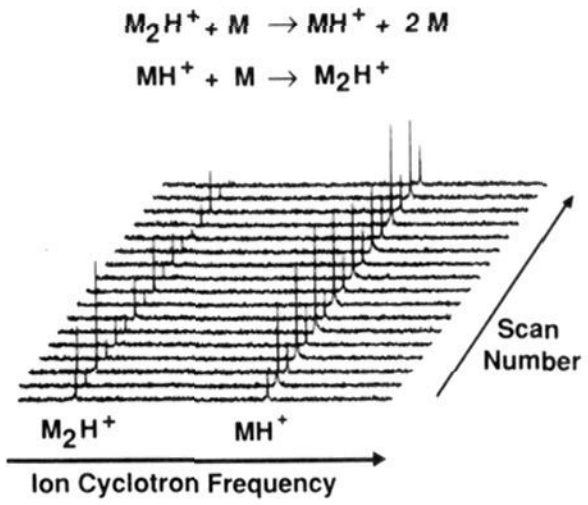

Figure 3. Portion of the acetone FT/ICR magnitude-mode frequency-domain spectrum prior to Fourier transformation in the second (parent ion radius modulation) dimension. The rapid modulation of the protonated acetone parent ion, MH^+, carries over to the observed ICR signal magnitude of the product ion, M_2H^+. (The slower modulation of protonated acetone dimer parent ion, M_2H^+, produces a less obvious modulation in the ICR signal magnitude of its MH^+ product ion.) These modulation transfers become apparent following a second FT of this data with respect to the modulation (here shown as "scan number") axis (see Figure 4).

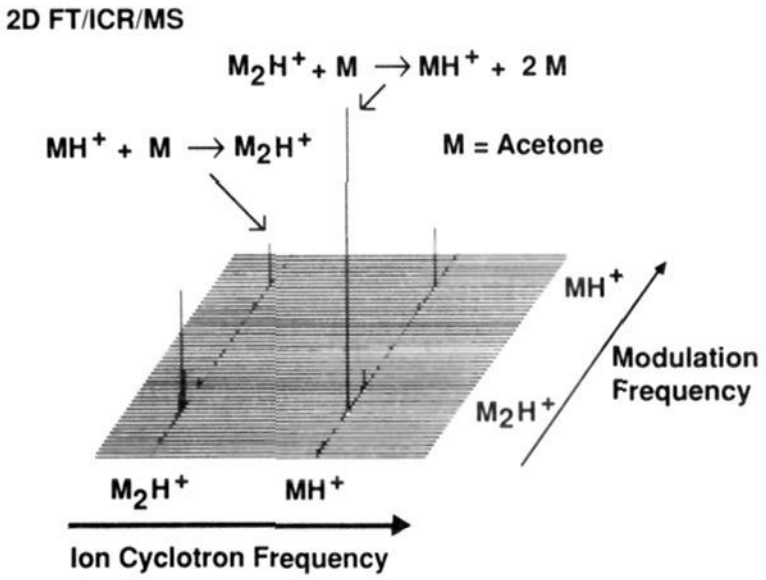

Figure 4. Three-dimensional stacked-plot display of a portion of the two-dimensional data obtained by padding the data of Figure 3 with an equal number (512) of zeroes in the modulation dimension, followed by Fourier transformation of the data with respect to that dimension. The diagonal peak at the cyclotron frequency of M_2H^+ is rather broad in the modulation dimension, likely due to inadequate pressure control of acetone throughout the experiment. Some "T_1-noise" is also noticeable as rows of small peaks at the cyclotron frequencies of MH^+ and M_2H^+ (see text).

$$M_2H^+ + N \rightarrow MH^+ + M + N \qquad (5)$$

to form MH^+ increases with increased M_2H^+ ion cyclotron radius (and thus ion speed). Therefore, modulation of the cyclotron radius of either MH^+ or M_2H^+ parent ions produces a modulation in the number of product M_2H^+ or MH^+ ions, respectively.

Figure 3 shows a stack plot of some of the 512 spectra, $S(t_1,\omega_2)$, following the first FT (with respect to t_2) in each row of a two-dimensional array of FT/ICR time-domain data, $s(t_1,t_2)$ for electron-ionized acetone. Two principal ionic species, protonated acetone, MH^+, and protonated acetone dimer, M_2H^+, are present in each spectrum, but the relative magnitude of each peak is modulated as one proceeds from one spectrum to the next.

The frequencies of that modulation are revealed by subjecting the data to a second FT with respect to the scan number as the second "time" axis (padded with 512 zeroes before FT), to yield the 2D-FT/ICR mass spectrum, $S(\omega_1,\omega_2)$, shown in Figure 4. The "autocorrelated" peaks rising along the diagonal from the lower left to the upper right of Figure 4 constitute the conventional one-dimensional FT/ICR parent ion mass spectrum, because the ICR orbital radius of a given parent ion just after the SWIM

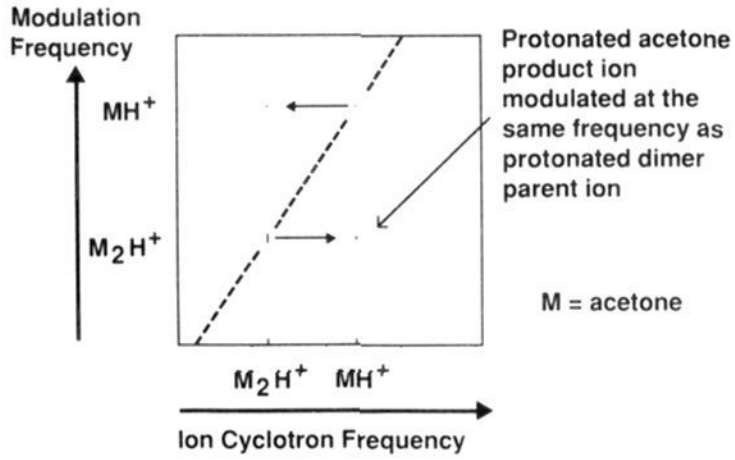

Figure 5. Two-dimensional isopower contour (SWIM) FT/ICR mass spectrum for ions derived from acetone. A peak appears on the diagonal (dashed) line for parent ions for each m/z value in the detected spectral bandwidth. Each off-diagonal peak results from a product ion (identified by vertical projection to the bottom horizonal axis) formed from a parent ion (identified by horizontal projection to the modulation frequency axis at the left of the figure). The small spot size for the various peaks results from the high mass spectral resolution under these experimental conditions (see text).

excitation period determines the subsequent ICR signal for that same parent ion observed after the second excitation. The off-diagonal peaks arise from ion-molecule reactions.

For example, we observe an off-diagonal peak (see lower right of Figure 4) if the modulated frequency is that of M_2H^+ and the detected ICR frequency is that of MH^+; in other words, modulation of the speed of M_2H^+ produces a modulation of the MH^+ abundance, establishing the "coupling" reaction $M_2H^+ \rightarrow MH^+$ (presumably collision-induced dissociation, as shown in Figure 4). Similarly, the off-diagonal peak at the upper left of Figure 4 establishes the presence of the "coupling" reaction $MH^+ \rightarrow M_2H^+$. The mirror-image off-diagonal peaks in Figure 4 are of unequal magnitude, because ion-molecule forward and reverse reactions are generally of unequal rate and may (as in this example) not even correspond to the same process.

The ion-molecule reaction pathways are visualized more directly if the data of Figure 4 are replotted as an isopower rectilinear 2D-contour plot (Figure 5), from which it is easier to see that modulation at the ICR frequency of M_2H^+ leads to an observed signal at the ICR frequency of MH^+, and vice versa. The diagonal along which the parent ion mass spectrum lies does not pass through the corners of the display, because of the unequal frequency ranges in the modulation (ν_1) and observed (ν_2) frequency dimensions. ν_1 has a frequency range of 924.75 kHz (i.e., not extending to 0 Hz) whereas ν_2 has a frequency range of 1.3333 MHz (which does extend to 0 Hz). The frequency range in the modulation dimension is determined by the range of excitation ($\nu_{high} - \nu_{low}$). Hence, diagonal peaks are observed at a position where $\nu_1 = \nu_2$.

The spurious peaks observed in the 3D stacked plot in the modulation frequency direction at the observed cyclotron frequencies of protonated acetone and its proton-bound dimer are due to variation in the number of ions from one event sequence to the next. Such variations arise from fluctuations in the neutral pressure of acetone in the vacuum chamber, as well as fluctuations in the electron beam current during the ionization event. This effect is analogous to the "T_1-noise" observed in 2D-FT/NMR,[68] arising from variations in spin populations from scan to scan.

Finally, in our experiments, the SWIM event excites ions to a radius of only about 17% of the trap radius. Thus, no ions are ejected, and the excitation is highly linear, as evidenced by the absence of harmonics along the modulation frequency axis.

Proton-Transfer Reactions: Pyrrolidine and 3-Methylpyridine. Our second experimental example (see 2D-SWIM FT/ICR MS/

(68) Freeman, R. *A Handbook of Nuclear Magnetic Resonance*; John Wiley & Sons: New York, 1987.

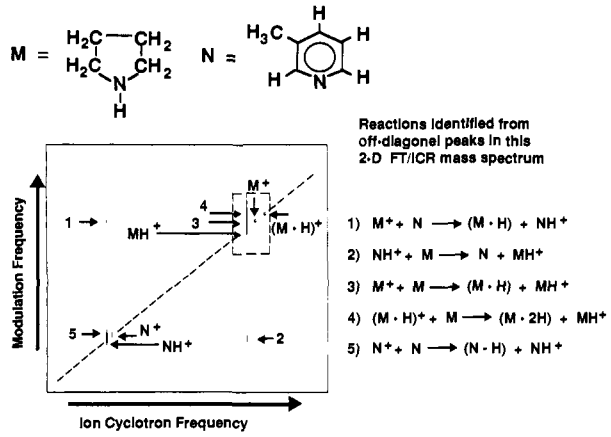

Figure 6. Stored-waveform ion modulation (SWIM) 2D-FT/ICR mass spectral isopower contours, from which five ion-molecule proton-transfer reactions of pyrrolidine and 3-methylpyridine may be identified (see text).

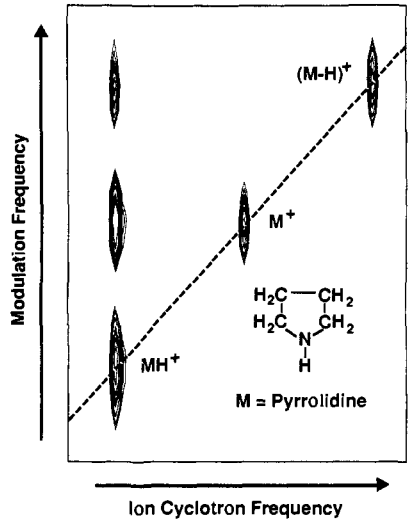

Figure 7. Narrow-band SWIM 2D-FT/ICR mass spectral isopower contours for the pyrollidine molecular ion region. Experimental conditions are as in Figure 6, except that the SWIM modulation (and excitation/detection) frequency bandwidths were narrowed to provide higher analog and digital resolving power.

MS contour plot in Figure 6) begins to show the power of the two-dimensional approach. Here we examine an electron-ionized mixture of two heterocyclic nitrogen-containing bases, pyrrolidine (M) and 3-methylpyridine (N). Ionization with low-energy electrons produces almost exclusively molecular ions, which are SWIM-modulated and then allowed to react for 150 ms at equal partial pressures (10^{-7} Torr total pressure) before broad-band excitation/detection. At least five distinct ion-molecule reactions are readily identified from the corresponding off-diagonal peaks in the 2D mass spectrum. It is important to note that all five ion-molecule reactions can be inferred *without any prior knowledge of the system.* The contour level shown was intentionally set low so that all peaks could be seen in a single display. Thus, the peaks in the vicinity of the cyclotron frequency of the protonated pyrrolidine ion appear unresolved but would in fact be resolved if the contour level were set higher.

Figure 7 shows the increased digital resolution resulting from repetition of the experiment for pyrrolidine alone (i.e., no 3-methylpyridine present), conducted over a narrower spectral bandwidth (corresponding to the area bounded by the dashed rectangle in Figure 6), from which the processes $(M-H)^+ \rightarrow MH^+$ and $M^+ \rightarrow MH^+$ are clearly resolved. As for one-dimensional FT/ICR/MS, one would usually perform a low-resolution experiment first, to determine the m/z range(s) for

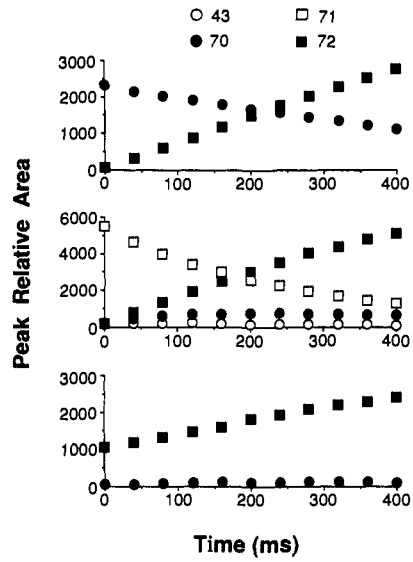

Figure 8. Time evolution of ions derived from pyrrolidine, based on one-dimensional FT/ICR mass spectra obtained at each of a series of reaction periods between ion formation by electron ionization and subsequent excitation/detection. Each data point represents an average of two peak area values.[58] The protonated molecular ion, $(M+H)^+$, is clearly a product of M^+ and $(M-H)^+$, whereas $(M+H)^+$ simply grows with time and does not form additional product ions. These results strongly validate our interpretation of the two-dimensional data in Figures 6 and 7.

which higher resolution is needed. Then, if necessary, one could "zoom" in on that range (i.e., narrower bandwidth and/or more data points/bandwidth) to achieve the needed mass-resolving power.

One-Dimensional Double-Resonance Confirmation of 2D-SWIM FT/ICR MS/MS Results. To confirm the reaction connectivities inferred from the SWIM 2D-FT/ICR MS/MS data shown in Figures 6 and 7 for ions derived from pyrrolidine, we carried out a series of conventional one-dimensional double-resonance experiments. Each of the pyrrolidine-derived ions, $(M-H)^+$, M^+, and $(M+H)^+$, was isolated in turn, and its reaction with neutral pyrrolidine was monitored from 0 to 400 ms in 40-ms increments. The data in Figure 8 (top) show that $(M-H)^+$ (m/z 70) disappears at the same rate as the protonated pyrrolidine ion, $(M+H)^+$ (m/z 72), is produced. Similarly, Figure 8 (middle) shows that the pyrrolidine molecular ion, M^+ (m/z 71), produces $(M+H)^+$, (m/z 72), and Figure 8 (bottom) shows that neither M^+ or $(M-H)^+$ is produced from $(M+H)^+$. Thus, the one-dimensional double-resonance results fully corroborate the ion-molecule reactions identified from the 2D mass spectra of Figures 6 and 7.

Fragmentation vs Ion–Molecule Reactions. A little reflection reveals that collision-induced fragmentation of parent ions will yield SWIM 2D-FT/ICR MS/MS peaks on only one side of the diagonal of the display. Some ion-molecule reactions, on the other hand, are reversible and can produce peaks on both sides of the diagonal. A particularly interesting application for this experiment might be MS/MS of multiply charged ions generated by electrospray ionization, because both the mass and charge of such ions can change during fragmentation; hence, fragment ions do not necessarily have lower m/z than their parent ions.

Radius Modulation vs Energy Modulation. In some endoergic reactions, e.g., collision-induced dissociation, a minimum-energy threshold must be overcome for a reaction to occur. Thus, a simple sinusoidal modulation of parent ion cyclotron radius from zero to (say) 50% of the trap radius will result in a "clipped" (i.e., distorted) sinusoidal modulation of the product ion abundance, resulting in nonlinear response, and introduction of signals at harmonic and combination frequencies. However, the problem is readily avoided by modulating the parent ion cyclotron radius

from a minimum value (by adding a constant to eq 3) chosen to correspond to a kinetic energy above the reaction energy threshold.

Moreover, ion-molecule reaction rates may vary directly with ion kinetic energy rather than with ion cyclotron radius.[65] Since ion kinetic energy varies as the square of ion cyclotron radius, a sinusoidal modulation of ion cyclotron radius will *not* produce a sinusoidal modulation of parent ion kinetic energy (or product ion abundance) in such a case. However, with stored-waveform ion modulation, it is possible to tailor the excitation profile so as to produce a sinusoidal modulation of ion kinetic energy as a function of cyclotron frequency, so that SWIM 2D-FT/ICR MS/MS could remain linear even in that situation. We denote the energy-modulation 2D experiment as SMOKE (stored-waveform modulation of kinetic energy).

Generality of the SWIM Method for 2D-FT/ICR MS/MS. Stored-waveform excitation includes all other excitation waveforms as subsets. Thus, for example, Hadamard FT/ICR MS/MS experiments[53] could be conducted as shown here, simply by tailoring a series of square-wave modulated (rather than sine-wave modulated) SWIM excitation spectra. Alternatively, one could tailor waveforms so as to eject undesired high-abundance ions throughout an experiment, by introducing a high-magnitude spike at the cyclotron frequency corresponding to each undesired m/z in the series of excitation spectra shown in Figure 2.

SWIM vs Excite–Delay–Excite for 2D-FT/ICR MS/MS. The present stored-waveform method offers several advantages over the original excite–delay–excite method.[39-41] First, broad-band excitation requires inconveniently small time increments in the variable-delay event of the excite–delay–excite sequence but is not a problem with SWIM. Second, with SWIM, we can more easily modulate the parent ion radius between two finite values. Third, sinusoidal modulation of ion kinetic energy (rather than ion cyclotron radius) requires SWIM. Fourth, the duration of the excitation event is fixed in SWIM but necessarily varies in excite–delay–excite; therefore, SWIM should provide a more accurate measure of ion–neutral collision and reaction products. Finally, SWIM excitation makes possible the introduction of mass "windows" for simultaneous ion modulation, ejection, and nonexcitation, for systems in which one wants to observe low-abundance ions in the presence of (less interesting) high-abundance ions.[69]

Equilibrium Constants from SWIM 2D-FT/ICR MS/MS. The reader will by now recognize that, for bimolecular processes, the relative magnitudes of the off-diagonal peaks in a SWIM 2D-FT/ICR MS/MS display are directly related to the respective ion-molecule reaction rate constants. Thus, just as it is possible to determine an ion-molecule reaction equilibrium constant as the ratio of the forward to reverse rate constants

$$K_{eq} = \frac{k_{forward}}{k_{reverse}} \qquad (6)$$

in the so-called "kinetic" method[70] for determining K_{eq}, we propose that the equilibrium constant for a reversible reaction could (with the same limitations as the one-dimensional kinetic method) be determined from the ratio of the areas[58] of the mirror-image peaks on either side of the diagonal of a SWIM 2D-FT/ICR MS/MS plot.

Phasing and Display of 2D-FT/ICR MS/MS Data. In the present work, we have performed a magnitude calculation after the first FT stage.[42] As a result, overlapped peaks in the spectrum can be expected to exhibit some distortion[71-73] which could be manifested as peaks at harmonic or combination frequencies following the second FT. However, in practice we do not typically see such spurious peaks, and magnitude-mode calculation is much simpler than phasing after the first FT.

The 2D mass spectral representations in Figures 5–7 are displayed as contours of constant power rather than contours of constant magnitude. As in 2D-FT/NMR,[74] it is convenient to use power spectral display, because the peaks are narrower than those in magnitude-mode display.[25] One should of course be aware that the relative peak heights in such a display are *not* linearly related to relative ion abundances (e.g., a peak of twice the magnitude will have four times larger power). However, for quantitative work, the relevant off-diagonal peak magnitudes can readily be extracted from the data.

In principle, phase-sensitive 2D FT/ICR MS/MS could make it possible to distinguish between ion-molecule reactions whose rates increase or decrease with increasing ion energy. We are investigating this possibility.

SWIM 2D-NOESY NMR. In the limit of very small "tip" angle, $\sin\theta \approx \theta$, NMR response amplitude becomes linearly proportional to excitation amplitude. Certain NMR pulse sequences are designed to take advantage of this linear limit.[75] Therefore, the method proposed here could be used to produce NOESY-type 2D/FT/NMR spectra, provided that the excitation modulation range was limited to small tip angles.

Conclusion

In summary, we have devised and demonstrated a fundamentally new scheme, based on the high linearity of the ICR experiment, for obtaining MS/MS data, multiplexed with respect to both parent and product ions. The method provides a simple graphical means for identifying all ion-molecule pathways simultaneously from a single automated experiment. Such capability should prove especially useful in analysis of complex mixtures containing a large number of overlapped peaks, as well as better controlled measurements of multiple equilibria (such as proton-transfer equilibria between an unknown and a series of reference bases) in a single experiment. With suitable precautions, it should prove possible to determine relative ion-molecule reaction rate constants and equilibrium constants from relative peak areas and peak area ratios for a whole family of interconnected reactions at once. Finally, the present method, although devised expressly for FT/ICR/MS, can be extended to 2D-NOESY NMR in the limit of small tip angle.

Acknowledgment. This work was supported by the U.S.A. National Science Foundation (Grant CHE-9021058), the U.S.A. Public Health Service (N.I.H. Grant GM-31683), and The Ohio State University.

(69) Chen, L.; Marshall, A. G. *Int. J. Mass Spectrom. Ion Processes* **1987**, *79*, 115–125.
(70) Nourse, B. D.; Cooks, R. G. *Int. J. Mass Spectrom. Ion Processes* **1991**, *106*, 249–272.
(71) Lee, J. P.; Comisarow, M. B. *J. Magn. Reson.* **1987**, *72*, 139–142.
(72) Lee, J. P.; Chow, K. H.; Comisarow, M. B. *Anal. Chem.* **1988**, *60*, 2212–2218.
(73) Wang, M.; Marshall, A. G. *Int. J. Mass Spectrom. Ion Processes* **1988**, *86*, 31–51.
(74) Bax, A. *Two-Dimensional Nuclear Magnetic Resonance in Liquids*; D. Reidel Publishing Co.: Dordrecht, Holland, 1982.
(75) Oschkinat, H.; Pastore, A.; Bodenhausen, G. *J. Am. Chem. Soc.* **1987**, *109*, 4110–4111.